Developmental Biology 399 (2015) 27–40

Contents lists available at ScienceDirect

Developmental Biology

journal homepage: www.elsevier.com/locate/developmentalbiology

A dual epimorphic and compensatory mode of heart regeneration in zebrafish

Pauline Sallin [1], Anne-Sophie de Preux Charles [1], Vincent Duruz, Catherine Pfefferli, Anna Jaźwińska *

Department of Biology, University of Fribourg, Chemin du Musée 10, 1700 Fribourg, Switzerland

ARTICLE INFO

Article history:
Received 22 August 2014
Received in revised form
27 November 2014
Accepted 3 December 2014
Available online 31 December 2014

Keywords:
Heart regeneration
Epimorphic regeneration
Blastema
Compensatory growth
Cell cycle
N2.261
Phosphohistone H3
Cardiac undifferentiated cells
Embryonic ventricular myosin
Zebrafish

ABSTRACT

Zebrafish heart regeneration relies on the capacity of cardiomyocytes to proliferate upon injury. To understand the principles of this process after cryoinjury-induced myocardial infarction, we established a spatio-temporal map of mitotic cardiomyocytes and their differentiation dynamics. Immunodetection of phosphohistone H3 and embryonic ventricular heavy chain myosin highlighted two distinct regenerative processes during the early phase of regeneration. The injury-abutting zone comprises a population of cardiac cells that reactivates the expression of embryo-specific sarcomeric proteins and it displays a 10-fold higher mitotic activity in comparison to the injury-remote zone. The undifferentiated cardiomyocytes resemble a blastema-like structure between the original and wound tissues. They integrate with the fibrotic tissue through the fibronectin-tenascin C extracellular matrix, and with the mature cardiomyocytes through upregulation of the tight junction marker, connexin 43. During the advanced regenerative phase, the population of undifferentiated cardiomyocytes disperses within the regenerating myocardium and it is not detected after the termination of regeneration. Although the blastema represents a transient landmark of the regenerating ventricle, the remaining mature myocardium also displays an enhanced mitotic index when compared to uninjured hearts. This suggests an unexpected contribution of a global proliferative activity to restore the impaired cardiac function. Based on these findings, we propose a new model of zebrafish heart regeneration that involves a combination of blastema-dependent epimorphosis and a compensatory organ-wide response.

Introduction

In mammals, the mitotic activity of cardiac muscle cells expires shortly after birth. Despite this postnatal switch from hyperplastic to hypertrophic growth, it is well accepted that adult cardiomyocytes (CMs) retain the ability to re-enter the cell cycle under various pathological and physiological conditions (Beltrami et al., 2001; Bergmann et al., 2009; Soonpaa and Field, 1998; Soonpaa et al., 2013). Recent findings have demonstrated that adult mammalian CMs can undergo partial dedifferentiation in order to cope with different pathological situations (Kubin et al., 2011; Rajabi et al., 2007; Taegtmeyer et al., 2010). CMs dedifferentiation provides the cellular plasticity to promote adaptive cardiac remodeling and to enhance survival under hypoxic conditions (Szibor et al., 2014). Nevertheless, these responses are insufficient to allow mammalian heart regeneration after acute myocardial infarction leading to defective healing with replacement of the dead myocardium with a collagen-rich scar. A growing ambition in the field of regenerative research is to boost a latent proliferative ability of CMs to stimulate heart regeneration in mammals. This concept has been largely inspired by the extraordinary cardiac regenerative capacity of non-mammalian vertebrates, such as amphibians or teleost fish (Ausoni and Sartore, 2009; Major and Poss, 2007; Singh et al., 2010; Yelon, 2012).

Zebrafish CMs remain responsive to mitogenic signals throughout their entire life (Kikuchi and Poss, 2012). This feature allows the zebrafish complete regeneration of functional heart tissue after ventricular injury. Indeed, a mutation of a mitotic checkpoint kinase *mps1* blocks cardiac restoration and it results in scarring (Poss et al., 2002). Recent studies using genetic fate-mapping experiments provided clear evidence that the new myocardium originates from the pre-existing CMs, which undergo dedifferentiation, re-enter the

Abbreviations: CM, cardiomyocyte; reg My, regenerated myocardium; ori My, original myocardium; embCMHC, embryonic cardiac myosin heavy chain, ECM, extracellular matrix; PIT, post-infarcted tissue; dpci, days post cryoinjury; CI, cryoinjury; MyoC, myocardium

* Corresponding author. Tel.: +41 263008890; fax: +41 263009741.
E-mail address: anna.jazwinska@unifr.ch (A. Jaźwińska).

[1] Equal contribution.

http://dx.doi.org/10.1016/j.ydbio.2014.12.002

cell cycle and ingrow into the area of the wound (Curado and Stainier, 2006; Kikuchi et al., 2010; Lepilina et al., 2006; Poss, 2007; Zhang et al., 2013). This plasticity of CMs has been located at the vicinity of the injury, suggesting the presence of a cardiogenic environment generated by the trauma (Lepilina et al., 2006). The regenerative contribution of the remaining myocardial wall, which is located distantly from the site of injury, still needs to be analyzed.

In vertebrates, two exclusive categories of reparative organ regeneration have been proposed, namely compensatory and epimorphic regeneration (Brockes and Kumar, 2008; Carlson, 2007). One of the significant differences between both processes is that in the compensatory mode, the proliferative response occurs throughout the remaining organ, whereas in epimorphosis, it is confined to the vicinity of the wound. The compensatory regeneration typically results in a regaining of functional mass, rather than a shape reproduction. A classic example of the compensatory regeneration has been reported for the mammalian liver, in which the remaining hepatic tissue enlarges, but the original parts do not grow back (Carlson, 2007). On the other hand, the hallmark of the epimorphic regeneration is an accurate reconstruction of the amputated structures without an enlargement of the organ remnant. Some distinctive examples of this mode of regeneration are urodele limbs and zebrafish fins, in which the growth of the new parts starts at the level of the amputation plane by the creation of a proliferative population of undifferentiated cells, called a blastema, underneath the wound epidermis (Brockes and Kumar, 2008). Similarly, the studies of the zebrafish ventricle resection model have suggested an epimorphic-like mode of heart regeneration (Lepilina et al., 2006). In this perspective, the activation of the epi-endocardium resembles the role of the wound epidermis during limb or fin regeneration. Indeed, shortly after the ventricular damage, epithelial and endocardial cells become active and proliferate. Moreover, these cells specifically communicate with CMs through different signaling pathways, such as FGF or retinoic acid (Kikuchi et al., 2011).

Our laboratory and others have previously developed a cryoinjury model in the zebrafish heart, which is characterized by enhanced cell proliferation, transient fibrosis and complete regeneration within one to two months (Chablais et al., 2011; Gonzalez-Rosa et al., 2011; Schnabel et al., 2011). However, unlike the amputation model, the immediate effects of cryoinjury simulate the cellular outcomes of mammalian myocardial infarction, such as massive cell death, inflammation, and scar deposition. Although the zebrafish cryoinfarction is of a particular value from the perspective of regenerative medicine, it has not yet been addressed whether the associated regenerative success occurs by epimorphic or/and compensatory responses. Moreover, several important questions concerning the role of cellular proliferation during this process remain open, such as (1) what types of cells are dividing, (2) where do the proliferation takes places, (3) what triggers the cell-cycle entry and (4) what is the ultimate contribution of the newly generated cells in the regenerated organ. Finally, a detailed analysis of the extent and importance of cellular dedifferentiation during the proliferative activity of CMs is still missing. Although the presence of a complex sarcomeric network could physically hamper the cytokinesis process (Jopling et al., 2011), it seems that it does not completely exclude a cell division activity in CMs (Engel, 2005; Laube et al., 2006; Zebrowski and Engel, 2013).

In zebrafish, most of the assessments of CM proliferation have been based on immunofluorescence analysis using G1/S phase markers. However, cell cycle re-entry can have several downstream consequences that are not necessary mitosis but also polyploidization and eventually binucleation, which are well-documented outcomes in the mammalian heart (Zebrowski and Engel, 2013). Although mitotic events have been observed in the initial study of zebrafish heart regeneration (Ahuja et al., 2007; Poss et al., 2002), the dynamic distribution of mitotic CMs has not yet been analyzed at the high-resolution after ventricular damage in zebrafish. Quantification of M-phase events is essential to determine a spatio-temporal dimension of proliferating CMs in order to distinguish between the local epimorphic and global compensatory stimulation of heart regeneration. The detailed characterization of the regenerative patterns is needed to recognize potentially distinct regulatory mechanisms that activate cardiac responses to injury.

In this study, we set out to establish a map of proliferating CMs during the main stages of ventricular regeneration. Using several distinct proliferation markers, we could assess both the cell cycle re-entry (G1/S phase) and the mitotic index (a transition to M-phase) of the same specimens. In addition, we monitored the level of CM differentiation through a detection of the embryo-specific myosin expression. These analyses identified a transient population of wound-associated undifferentiated CMs, which resemble a cardiac blastema. Although cellular proliferation was the highest in the cardiac blastema, we observed an enhanced global induction of cell division within the entire myocardium, suggesting a compensatory response of the heart. In the myocardium beyond the blastema, the mitotic activity of CMs occurred without a reactivation of the embryonic myosin gene. Thus, the mature zebrafish CMs do not require a gross modification of their structural differentiation status in order to enter the cell cycle. According to these new data, we propose that heart regeneration in zebrafish is achieved by a dual mechanism involving an initially formed population of immature cardiac blastema cells in parallel to proliferating mature CMs. Integration of both regeneration modes (epimorphic and compensatory) ensures an efficient functional recovery of this life-essential organ after injury.

Results

Assessment of the G1/S-phase and mitotic activities of cardiomyocytes during heart regeneration

One of the suitable markers of G1/S-phases is represented by Minichromosome Maintenance Complex Component 5 (MCM5), a protein that serves to unwind DNA during replication and to regulate centrosome duplication in eukaryotic cells (Knockleby and Lee, 2010). Using this marker, we have already demonstrated that cardiomyocyte (CM) cell-cycle entry is highly enhanced during heart regeneration after cryoinjury (Chablais and Jazwinska, 2012b; Chablais et al., 2011). However, the mitotic index in the regenerating zebrafish heart has not yet been determined. Here, to examine mitotic CMs, we used antibodies against phospho-(Ser10)-histone H3 (PH3), which demarcates condensed chromosomes (Hans and Dimitrov, 2001). Both proliferation markers, MCM5 and PH3, do not co-localize, because they are specific for the non-overlapping phases of the cell cycle. We first set out to provide a high resolution imaging of PH3 immunostaining during heart regeneration of the transgenic fish expressing EGFP under the control of cardiac specific promoter *cmlc2*. To detect EGFP in the nuclei of CMs, we immunostained the sections with anti-GFP antibody. The co-localization between the cardiac EGFP and PH3 signals was validated using the orthogonal projections (Fig. 1G–I). Remarkably, the pattern of PH3 immunostaining was often fragmented within the cell, indicating a segregation of condensed chromosomes during the nuclear division (Fig. 1C and F). To further validate the mitotic process in CMs, we visualized a centrosome marker γ-tubulin, which is normally enriched in the spindle apparatus during mitosis (Kollman et al., 2011; Lajoie-Mazenc et al., 1994). As expected, the PH3-positive CMs exhibited a strongly upregulated γ-tubulin expression (Suppl. Fig. 1). The partial co-localization of both markers indicates that the condensed chromosomes interact with the spindle apparatus. Collectively, these analyses provide high-resolution imaging of mitotic markers in adult zebrafish CMs in vivo.

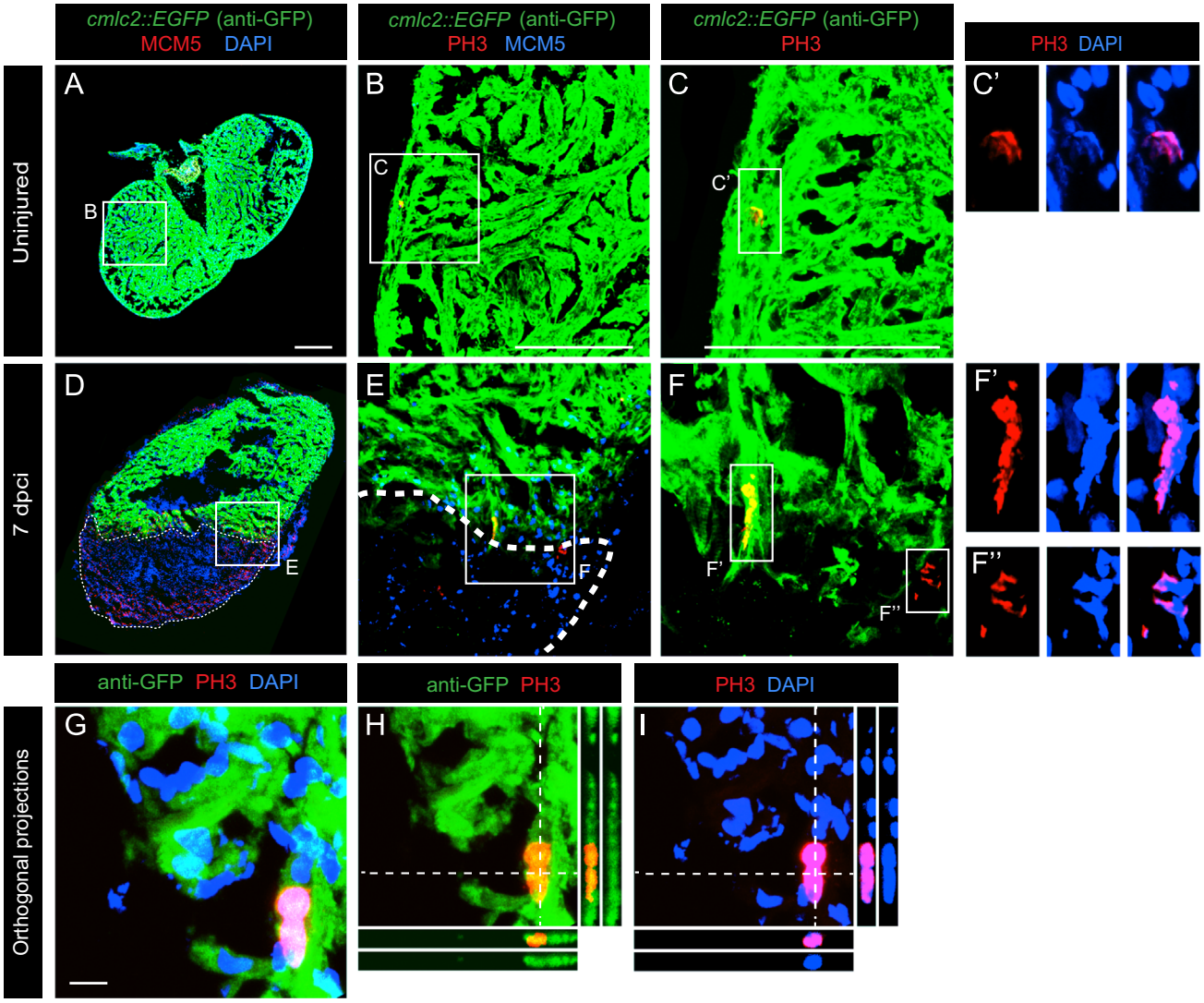

Fig. 1. Determination of the G1/S-phase and the mitotic indexes of cardiac and non-cardiac cells in the zebrafish ventricle. Heart sections were quadruple labeled using DAPI (nuclei) and antibodies against GFP (*cmlc2::EGFP*, cardiac cells), MCM5 (G1/S-phase) and PH3 (mitosis). (A–C) Uninjured heart contains a few proliferating cells. (B–C) Single PH3-positive mitotic cell (red) within the intact myocardium demarcated by GFP (green). (C') Higher magnification of the framed area in (C) with an overlap between PH3 (red) and DAPI (blue). (D–I) Heart at 7 dpci displays enhanced cell proliferation in both the post-infarction area and the remaining myocardium. (E, F) PH3-positive mitotic cells (red) at the injury border in the myocardium (green) and in the post-infarcted tissue (GFP-negative, black). (F',F") Higher magnification of the framed areas in (F) with an overlap between PH3 (red) and DAPI (blue). Fragmented pattern of nuclear staining reveals mitotic segregation of condensed chromosomes. (G–I) Representative image of a mitotic cardiac cell. Orthogonal projections demonstrate a co-localization between PH3 (red), GFP (green) and DAPI (blue) staining. Scale bars in (A, B, C)=100 μm; in (G)=10 μm.

To determine the rate of proliferating cells, we performed quadruple staining with DAPI, anti-GFP antibody (to enhance the endogenous *cmlc2::EGFP* in the cardiac nuclei), MCM5 and PH3 during the subsequent regenerative phases as compared to control uninjured hearts. The nuclei of CMs were distinguished from non-CMs by the presence of anti-GFP and DAPI staining (Fig. 1F). In both cell types, G1/S phase and mitosis were detected by MCM5 or PH3 immunostaining, respectively. In order to obtain convincing statistical data, we imaged and analyzed multiple non-adjacent sections of at least 5 hearts per time point, which resulted in a total score of approx. 150,000 CMs in each group (Table 1). The regenerative process is manifested by the replacement of the fibrotic tissue with a new myocardium, and consequently a decrease of the infarcted area relative to the entire ventricle (Chablais et al., 2011; Gonzalez-Rosa et al., 2011; Schnabel et al., 2011). At the onset of regeneration at 7 dpci, an average infarct size was 29 ± 7% of the ventricle sections (Table 1; Column: post-infarcted area). During the progression phase at 17 dpci, the fibrotic area was diminished to 9 ± 6.5% of the ventricle, and it was nearly completely resolved at 30 dpci (Table 1). This efficient regenerative process was associated with a remarkable proliferative activity of CMs, as compared to the uninjured ventricles that contained approx. 1% of MCM5-positive CMs and 0.01% of PH3-positive CMs (Fig. 1A–C; Fig. 2A and C). Although the value of 0.01% appears very low, the identification of a few mitotic CMs in the intact tissue suggests that the adult zebrafish ventricle undergoes a slow homeostatic tissue turnover under normal conditions.

As expected, the regeneration process was characterized by enhanced CM proliferation. At 7 dpci, nearly 12% of CMs were labeled with MCM5 and 0.04% of CMs displayed PH3-immunostaining (Fig. 2A and C). During the progression phase at 17 dpci, the number of MCM5-positive CMs declined by a half in comparison to the initiation phase (nearly 6%), and the number of PH3-positive cells slightly decreased (0.03%) (Fig. 2A and C). During the termination phase at 30 dpci, mitotic events declined to the uninjured control level, although the number of MCM5-positive CMs remained significantly higher than in uninjured heart (Fig. 2A and C). Thus, the dynamics of CM proliferation correlated with the progressive replacement of fibrotic tissue (Table 1).

Table 1
Numbers of PH3- and of MCM5-positive cells among cardiomyocyte and non-cardiomyocyte populations of uninjured hearts and at different phases of regeneration. H, the heart from one fish; dpci, days post cryoinjury.

Days post cryo-injury	Heart (♯ of sections)	Cardiomyocytes		Non-cardiomyocyte cells		Post-infarcted area
		MCM5 +	PH3 +	MCM5 +	PH3 +	
Uninjured	H1 (15)	345/40819 (0.84%)	4/40819 (0.010%)	123/21505 (0.57%)	4/21505 (0.019%)	–
	H2 (16)	235/26783 (0.88%)	4/26783 (0.015%)	92/9449 (0.97%)	3/9449 (0.032%)	–
	H3 (14)	286/43950 (0.65%)	3/43950 (0.007%)	163/13358 (1.22%)	1/13358 (0.007%)	–
	H4 (11)	756/34088 (2.2%)	3/34088 (0.009%)	427/14912 (2.86%)	7/14912(0.047%)	–
	H5(6)	46/12627 (0.36%)	1/12627 (0.008%)	22/2942 (0.75%)	0/2942 (0%)	–
TOTAL		**1668/158267**	**15/158267**	**827/62166**	**15/62166**	
7 dpci	H1 (10)	2878/25252 (11.4%)	17/25252 (0.067%)	5412/70547 (7.67%)	64/70547 (0.09%)	41%
	H2 (6)	1879/16351 (11.49%)	5/16351 (0.031%)	1242/28671 (4.33%)	15/28671 (0.052%)	24.7%
	H3 (5)	1244/17576 (7.08%)	3/17576 (0.017%)	2163/42797 (5.05%)	31/42797 (0.072%)	22.5%
	H4 (4)	725/7751 (9.35%)	4/7751 (0.052%)	3512/58395 (6.01%)	67/58395 (0.115%)	28.1%
	H5 (9)	2118/34803 (6.09%)	13/34803 (0.037%)	2973/38439 (7.73%)	23/38439 (0.06%)	23.2%
	H6 (10)	5055/42542 (11.88%)	12/42542 (0.028%)	3734/59564 (6.27%)	65/59564 (0.109%)	32.7%
TOTAL		**13899/144275**	**54/144275**	**19036/298413**	**265/298413**	
17 dpci	H1 (6)	1689/26317 (6.42%)	6/26317 (0.023%)	485/17031(2.85%)	6/17031 (0.035%)	4.9%
	H2 (5)	1253/21906 (5.72%)	5/21906 (0.023%)	588/13261 (4.43%)	4/13261 (0.03%)	18.5%
	H3 (6)	1893/40625 (4.66%)	21/40625 (0.051%)	876/22783 (3.84%)	16/22783 (0.07%)	1.8%
	H4 (5)	384/27936 (1.37%)	2/27936 (0.007%)	649/18849 (3.44%)	4/18849 (0.02%)	15.1%
	H5 (6)	2232/29015 (7.69%)	5/29015 (0.017%)	1131/17093 (6.62%)	5/17093 (0.029%)	3.4%
TOTAL		**7451/145799**	**39/145799**	**3729/89017**	**35/89017**	
30 dpci	H1 (6)	1513/29007 (5.22%)	0/29007 (0%)	866/23739 (3.65%)	1/23739 (0.004%)	0.4%
	H2 (6)	926/20685 (4.48%)	8/20685 (0.039%)	384/13284 (2.89%)	3/13284 (0.022%)	–
	H3 (4)	410/12802 (3.2%)	1/12802 (0.008%)	456/10605 (4.3%)	1/10605 (0.009%)	–
	H4 (6)	1373/59295 (2.32%)	5/59295 (0.008%)	745/23075 (3.23%)	3/23075 (0.013%)	–
	H5 (5)	292/26967 (1.08%)	1/26967 (0.004%)	96/9135 (1.05%)	3/9135 (0.032%)	–
TOTAL		**4514/148756**	**15/148756**	**2547/79838**	**11/79838**	

Although CM proliferation was the main focus of our study, we also analyzed the mitotic response of non-cardiomyocytes (non-CMs) that are present in the heart. As expected, we detected enhanced cell division of non-CMs during heart regeneration, especially in the cryoinjured area (Fig. 1D and F"; Fig. 2B and D; Table 1). This indicates a rapid proliferation of non-cardiac cells that are most likely involved in repair of the damaged area.

The co-labeling with MCM5 and PH3 allows evaluating the relative duration and the incidence frequency of the G1/S phases and mitosis in the same specimens. Accordingly, we evaluated the proportion of PH3-positive cells among all proliferating cells (PH3-positive and MCM5-positive cells) in both CM and non-CM cell populations. The obtained values were very low, ranging from 0.004 to 0.016, indicating that the mitosis was detected from 60- to 250-times less frequently than the G1/S phases (Fig. 2E). For non-CMs, a similar ratio of mitosis among the cycling cells was maintained in the uninjured and regenerating heart. By contrast, the CMs of the injured hearts exhibited different cycling characteristics than the CMs of control hearts. Surprisingly, the highest fraction of PH3-positive CMs was observed in uninjured hearts (0.013%), and this value dropped by 3-folds in the regenerating hearts at 7 and 30 dpci, or by nearly 2-folds at 17 dpci (Fig. 2E). Thus, the regenerating hearts contained a fraction of CMs that enter the cell cycle but do not complete the transition into the M-phase. This finding suggests a difference in the regulation of the cell cycle between the homeostatic conditions and the injury-triggered regeneration.

Mapping of mitotic CMs suggests epimorphic and compensatory mode of heart regeneration

To determine the spatial distribution of all individual dividing CMs during heart regeneration, we measured and plotted the shortest distance from each of the PH3-positive cardiac cell relative to the injury border (Fig. 3A and B). During the initiation phase at 7 dpci, the frequency of mitosis in the myocardium displayed a graded distribution, in which the area between 0 and 100 μm from the cryoinjury border encompassed 50% of the total number of PH3-positive CMs, the area from 100 to 200 μm contained 20% of these cells, and the remaining myocardium from 200 to 1000 μm comprised only 30% (Fig. 3C and D). This gradient indicates that the majority of all mitotic CMs are located at the vicinity of the wounded area, suggesting an influence of local injury-dependent mitogenic factors. However, beyond this area, the remaining myocardium contained evenly dispersed proliferating CMs, and no graded distribution from the injury border has been observed (Fig. 3B and D). Thus, the distance of approximately 100–200 μm from the border represents a landmark between the injury-associated highly proliferative zone and the original myocardium with lower and constant CM proliferation. Importantly, such a landmark was not detected during the progression phase at 17 dpci. The PH3-positive cells were nearly evenly spaced within the entire myocardium respectively to the injury boundary (Fig. 3B). Thus, the graphical representation of the spatial distribution of mitotic CMs revealed an unexpected difference between hearts at 7 and 17 dpci. Based on this plot, we concluded that the proximity of the injury zone enhances the rate of CM mitosis during the initial phase of regeneration, but not during the progression phase. Moreover, the dispersed distribution of PH3-positive CMs within the original myocardium at both time points suggests a contribution of systemic factors in stimulation of CM proliferation during heart regeneration.

To further determine the mode of CM proliferation, we labeled DNA-replicating cells with BrdU during 3 weeks starting at 7 dpci until 30 dpci of transgenic fish expressing nuclear DsRed under *cmlc2* promoter. This period corresponds to the post-inflammatory/wound healing phase, when the infarcted area becomes rapidly replaced with the new myocardium. At 30 dpci, the position of the original wound is not histologically recognizable due to the efficient integration of the

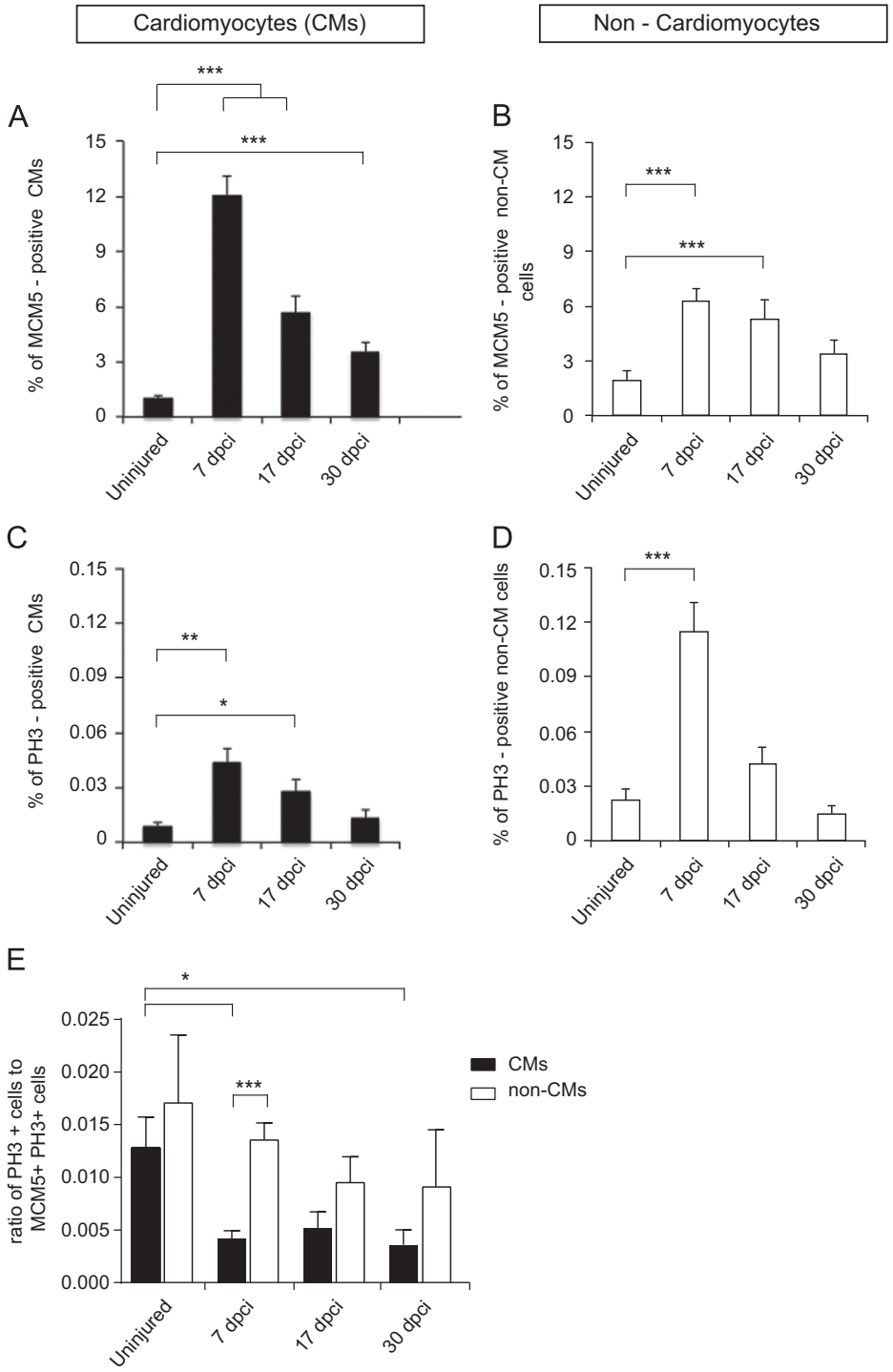

Fig. 2. Quantification of cell-cycle entry and mitosis of CMs and non-CMs during heart regeneration. Bar graphs of proliferating cells of uninjured and regenerating hearts at 7, 17 and 30 dpci. For each graph, the normalizations were done either with the total number of CMs or the total number of non-CMs. (A,B) Fraction of MCM5-positive CMs (A) and non-CMs (B). (C,D) Percentage of PH3-positive CMs (C) and non-CMs (D) cells. (E) The ratio of PH3-positive cells among all proliferating cells ($PH3^+$/($PH3^+ + MCM5^+$)) in the CMs and non-CMs populations reveals the fraction of mitosis relative to G1/S phase. All results are expressed as the mean ± standard error of the mean (S.E.M.) ($n \geq 5$ hearts; 4–15 sections per heart; $*P < 0.05$, $**P < 0.01$, $***P < 0.001$).

regenerate with the original tissue. Nevertheless, we inferred the position of the new myocardium based on the abundant BrdU labeling (Fig. 4C and D). We quantified the BrdU-positive cardiac nuclei in the regenerated myocardium (Reg My) and in the subsequent 100 µm-wide zones of the original myocardium (Ori My; Fig. 4F). We found that the majority (approx. 65%) of CMs located in the regenerated myocardium were BrdU-positive, supporting a notion that new cardiac tissue derives from newly generated cells. In the adjacent myocardial region (0–100 µm from the Reg My), we detected 30% of BrdU-labeled CMs. However, beyond this zone, all remaining subregions displayed approx. 10% of BrdU-containing CMs, demonstrating an even distribution of DNA-synthesizing cardiac cells within the original myocardium (Fig. 4F). Importantly, the fraction of the BrdU-labeled cells in the original ventricle was 2.8-fold higher than in uninjured hearts, which contained only 3.7% of BrdU-labeled CMs (Fig. 4A, E and F). The enhanced CMs proliferation in the entire

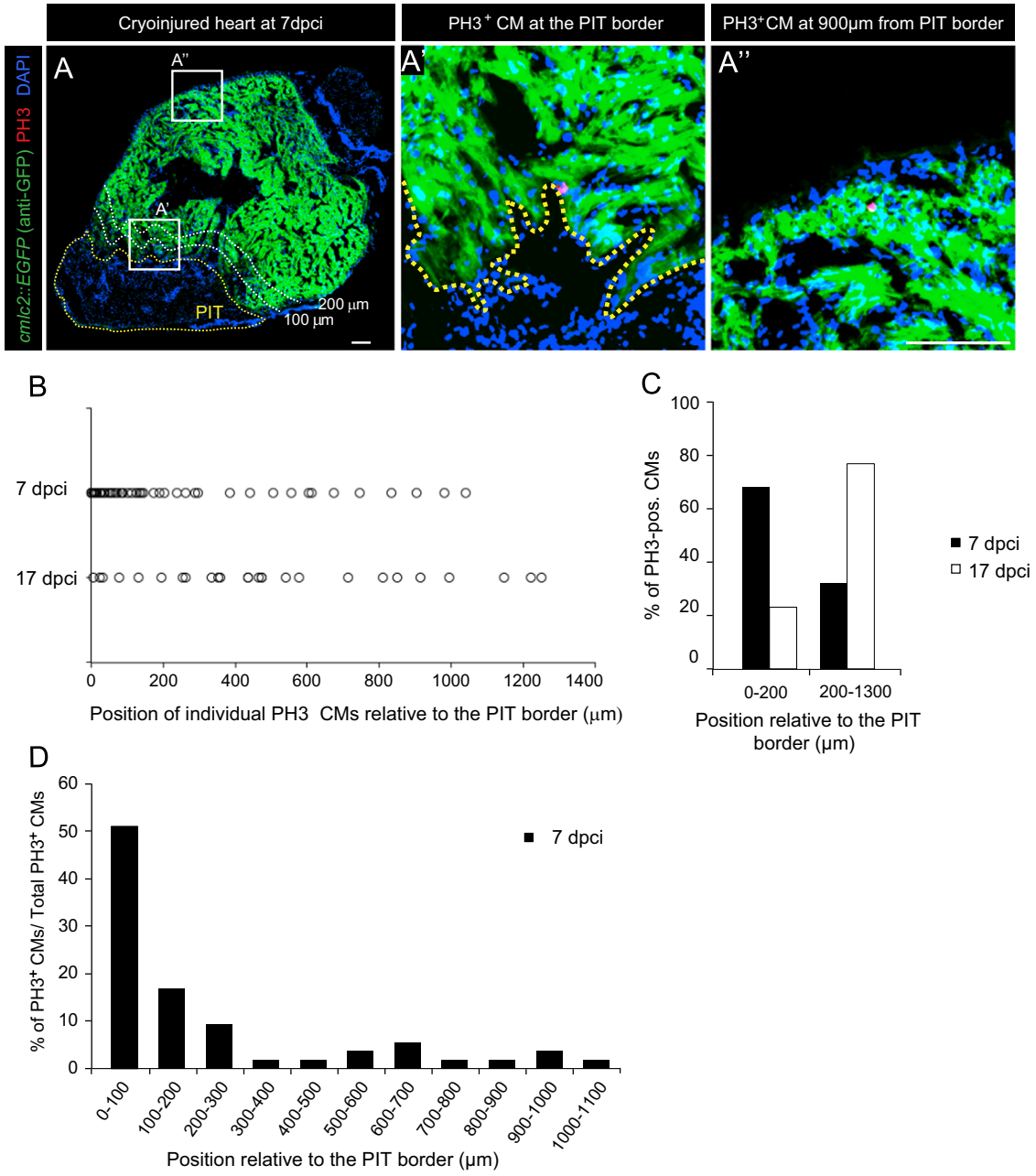

Fig. 3. Spatio-temporal distribution of PH3-positive CMs reveals two regenerative patterns in response to myocardial infarction. (A) Representative section of the heart at 7 dpci that was used for mapping PH3-positive cells (red) in the myocardium (green) in respect to the post-infarcted tissue (PIT; encircled by the yellow dotted line). Two zones of the myocardium at a distance of 0–100 and 100–200 µm from the PIT border are indicated with white dotted lines that are labeled with 100 µm and 200 µm, respectively. (A',A") Higher magnifications of the framed area in (A) showing PH3-positive cells at different distances from the PIT border. Scale bar (A, A")=100 µm. (B) Plot of the spatial distribution of PH3-positive CMs relative to the PIT border at 7 (n=53 cells) and 17 dpci (n=26 cells). (C) Fractions of PH3-positive CMs in the zones located in the proximity of PIT border (0–200 µm) or at distant locations from the site of injury (200–1300 µm) at 7 and 17 dpci. (D) Fractions of PH3-positive CMs in all the myocardial subdomains at 7 dpci demonstrate a graded distribution in the injury-abutting zone (0–200 µm) and an even distribution in the injury-remote zone (200–1300 µm).

original intact myocardium (the zones between 200–500 µm) suggests the presence of a systemic compensatory mode of heart regeneration, which acts in addition to the local injury-dependent mechanism.

The reactivation of embryonic cardiac sarcomeric proteins demarcates a highly proliferative cardiac blastema at the initial stage of heart regeneration

Previous studies have reported the downregulation of the *cmlc2* reporter and the partial loss of sarcomeric structures at the edge of myocardium close to the amputation plane of the resected ventricle (Jopling et al., 2010; Lepilina et al., 2006). Although these findings suggested the existence of undifferentiated CMs that resembled a blastema, the concept was not further reinforced with additional molecular evidence of an undifferentiated state of CMs underneath the wound. Here, to determine whether heart regeneration in zebrafish involves formation of immature CMs, we screened for antibodies that react with the early embryonic ventricle but not with the adult heart. We identified that such reactivity has a monoclonal antibody N2.261, which was raised against a mammalian neonatal muscle, and which binds the N-terminal end of slow β/cardiac MyHC (Jazwinska et al., 2003; Maggs et al., 2000). We tested this antibody at different developmental stages of zebrafish.

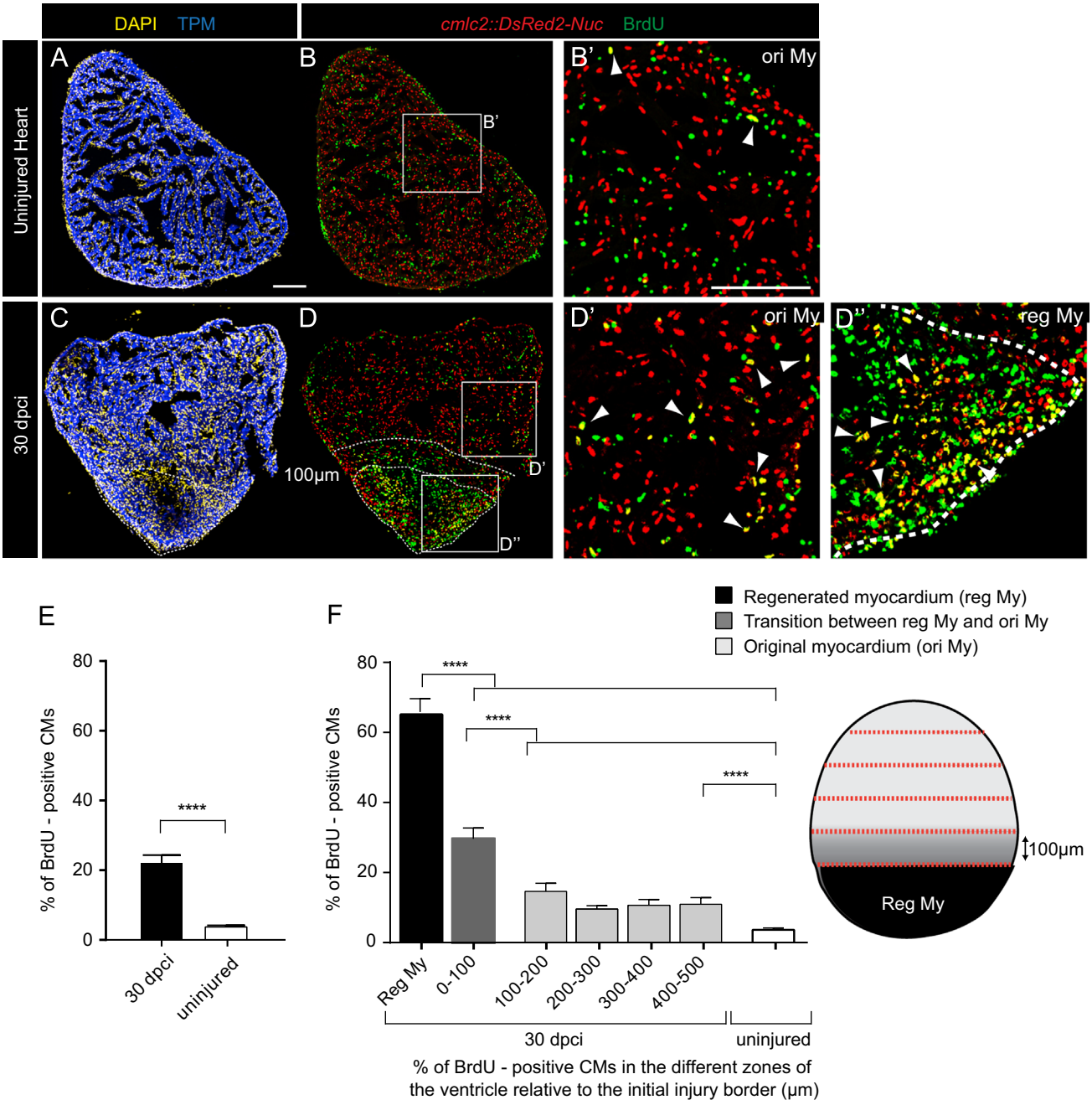

Fig. 4. Spatial distribution of BrdU-labeled CMs after the completion of heart regeneration demonstrates the local and global patterns of the proliferative activity. (A–D) Heart sections of uninjured *cmlc2::DsRed2-Nuc* transgenic zebrafish treated with BrdU for 21 days (A, B) and at 30 dpci after BrdU treatment from day 7 to day 30 (C, D). The expression of cardiac marker Tropomyosin (TPM blue) and Ds-Red-Nuc reveals nearly complete regeneration of the myocardium at 30 dpci (C, D). CMs after DNA synthesis were identified in both groups by the colocalization of BrdU and dsRed signals (B', D', D", arrows). (D, D', D") The border between the regenerated myocardium (reg My) and the original myocardium (ori My) can be identified by the difference in the BrdU incorporation (green). The region with abundant BrdU-labeling corresponds to the regenerated myocardium (encircled by a white dotted line). The most adjacent zone at 100 µm from this area is indicated with dashed line. Scale bar (A, B')=100 µm. (E) Quantification of BrdU-positive CMs in the entire regenerated heart at 30 dpci and in the uninjured control. (F) Quantification of BrdU-positive CMs in the reg My and in the 100 µm subregions of the ori My compared to uninjured heart. All results are expressed as the mean ± standard error of the mean (S.E.M.) ($n \geq 5$ hearts; 3–5 sections per heart; **** *P*-value < 0.0001).

In the embryo at 1 dpf, N2.261 co-localized with all *cmlc2::EGFP, cmlc2::DsRed2-Nuc* positive cells (Suppl. Fig. 2A and B). At 3 dpf, the immunoreactivity was detected in the embryonic ventricle but not the atrium (Suppl. Fig. 2C and D). During the larval stage at 12 dpf, the antigen of N2.261 was no longer expressed in the outer compact cell layer of the myocardium, but it was present in a subset of CMs in the central trabecular part of the ventricle (Suppl. Fig. 2E and F). This developmental switch of the N2.261 reactivity from the outer to inner layer of the ventricular wall reveals a migratory nature of the early embryonic CMs, which are known to delaminate from the primordial compact layer to establish the central trabecular myocardium of the zebrafish larval heart (Liu et al., 2010). This spatio-temporal dynamics support the notion that the N2.261-positive cells possess a morphogenetic plasticity that contributes to the pattern formation of the developing myocardium.

In the juvenile fish at 30 dpf, the ventricle did not express the antigen of N2.261, although some of the skeletal muscles remained strongly labeled with this antibody, providing an internal positive

control for the immunostaining procedure (Suppl. Fig. 2G and H). Thus, N2.261 antibody is specific for an early embryonic sarcomeric protein that becomes down regulated in the larval heart after a transition from the compact to the trabecular layer of the ventricular wall. We concluded that the antigen of N2.261 represents a structural marker of the embryonic undifferentiated CMs that have the migratory and developmental competences for heart morphogenesis. Based on this spatio-temporal analysis, we subsequently refer the corresponding antigen of N2.261 as embryonic cardiac myosin heavy chain (embCMHC) and we define the N2.261-positive CMs as cardiac undifferentiated cells.

To investigate whether the heart regeneration involves reactivation of embCMHC, we performed N2.261 antibody staining of hearts from the *cmlc2::EGFP* transgenic fish at 4, 7, 10, 17 and 30 dpci. At 4 dpci, a few embCMHC-positive cardiac fibers were detected at the injury border within a distance of up to 100 μm from the post-infarcted tissue (Fig. 5A). This localized expression pattern became more evident at 7 and 10 dpci (Fig. 5B and C). No embCMHC expression was observed in the original myocardium located beyond this leading-edge zone. Importantly, the N2.261-positive cells displayed lower levels of *cmlc2::EGFP* expression in comparison to the remaining myocardium (Fig. 5B and C), which is reminiscent of the study reporting an apical blastema after ventricular resections (Lepilina et al., 2006). In this regard, we tested the expression of embCMHC in the hearts after ventricular apex amputation, which is the classical injury model (Poss et al., 2002). Analysis of hearts at 7 dpa (days post amputation) revealed the presence of embCMHC-positive in a cluster-like domain along the wound margin (Suppl. Fig. 3). We concluded that at the onset of regeneration, irrespectively of the injury model, a pool of undifferentiated cardiac cells is established between the wound tissue and the remaining heart muscle.

During the progression phase at 17 dpci, the embCMHC-positive fibers lost their initial homogenous alignment along the injury margin, and they intermingled with the mature cardiac tissue of the regenerating myocardium (Fig. 5D). Thus, the transition from the early to advanced regeneration stage involves a reorganization of cardiac undifferentiated cells from the original distinct population at the leading edge to a more dispersed pattern that mixes with mature muscle fibers. This indicates an efficient integration of the undifferentiated CMs in the mass of the regenerating ventricle during the replacement of the fibrotic tissue. At 30 dpci, N2.261-reactivity was nearly absent, it could only be observed in a few remnant fibers (Fig. 5E). Taken together, these data suggest that the undifferentiated CMs are generated at the leading edge of the dedifferentiating adult myocardium during the initial phase of heart regeneration, and they provide a source of new mature CMs during progressive scar replacement. This spatio-temporal pattern of undifferentiated cardiac cells suggests a role of diffusible factors from the injury area during the upregulation of embCMHC in the adult ventricle after infarction. The creation of undifferentiated CMs at the interface between the adult original and infarcted tissues support a previously proposed concept of a cardiac blastema in zebrafish heart regeneration (Lepilina et al., 2006).

One of the key features of the blastema is the localized assembly of undifferentiated cells between the stump and wound tissue. To accurately determine the position of embCMHC–positive cells relative to the fibrotic tissue, we visualized the infarction zone at 7 dpci using antibodies against Fibronectin and Tenascin C (Chablais and Jazwinska, 2012b). The immunostaining revealed that the undifferentiated CMs were aligned along the extracellular matrix (ECM) fibers of the post-infarcted area (Fig. 6A-D). The relative expression pattern of both matrix proteins and embCMHC suggests that the juxtaposition of the fibrotic tissue with the adult myocardium could be a prerequisite for an activation of the embryonic cardiac genes in the cells along the wound plane.

To determine whether the undifferentiated CMs remain functionally integrated with the intact myocardium, we visualized the tight junctions using Connexin 43 as a marker. The immunostaining of heart sections at 7 dpci demonstrated a strong upregulation of Connexin 43 in the embCMHC-positive cells and in the adjacent embCMHC-negative CMs (Fig. 6E and F). This enhanced expression of a tight junction protein suggests a functional integration between undifferentiated and mature CMs in the cardiac blastema.

The blastema cells are typically highly proliferative. To determine the proliferation rate of undifferentiated and mature CMs in the regenerating hearts, we scored MCM5 positive cells in each of the domains at 7 dpci, and we found that 30% of cells in the embCMHC-positive domain were also expressing MCM5 (Fig. 7A, B and E). This fraction of proliferating cells was three-fold higher than in the remaining embCMHC-negative myocardium (Fig. 7E). Thus, upregulation of the embryonic cardiac gene is associated with a more rapid cellular proliferation at the onset of heart regeneration. Nevertheless, the low proportion (10%) of proliferating cells in the embCMHC-negative myocardium suggests that the activation of the embryonic program is not a prerequisite for the cell cycle entry.

To further verify this conclusion, we scored proliferating cells of regenerating ventricles at 17 dpci (Fig. 7C and D). During the advanced phase of regeneration, most of the hearts (4 hearts out of 6) displayed a markedly reduced embCMHC expression, and in these ventricles the difference of the proliferating cells between embCMHC-positive and -negative myocardium was not significant (Fig. 7F). We concluded that although the reactivation of the embryonic program facilitates the cell-cycle re-entry, it is not a prerequisite for the cell cycle entry. The mature CMs of the intact myocardium also possess the proliferative capacity that is stimulated during heart regeneration.

Discussion

A hallmark of cardiac regeneration in zebrafish is the capacity of endogenous CMs to proliferate upon injury. However, wrong associations between G1/S-phase detection and mitotic events often lead to incorrect estimation of CMs division activity (Engel, 2005; Zebrowski and Engel, 2013). In this study, we provide a quantitative analysis of both, DNA-replicating and mitotic cells after cryoinjury of the same specimens. The detection of Ser10-phosphorylated histone H3 (PH3) clearly demonstrated that mitosis is a very rare event, and multiple specimens need to be scored to obtain statistically significant data. Among approximately 150,000 CMs analyzed in uninjured hearts and at 7, 17 and 30 dpci, only 15, 54, 39 and 15 mitotic cardiac nuclei could be identified, respectively (Table 1). These values were 60 to 250-times lower than the frequency of the CMs in the G1/S-phase detected by MCM5 expression. The ratio of PH3-positive CMs among all proliferating (PH3- plus MCM5-positive) CMs revealed an unexpected difference in the cycling characteristics between uninjured and regenerating hearts. In comparison to uninjured hearts, this ratio was reduced by 2- to 3-folds at different time points after cryoinjury, indicating that the regenerative response is characterized by a lower rate of mitosis relative to the initiated cell-cycle entry. A plausible explanation for this result is that myocardial infarction massively stimulates CMs to enter the cell cycle, but some of these activated cells fail to efficiently progress into the mitotic phase. This suggests that some intrinsic factors could inhibit the transition to the M-phase under the pathological conditions. Studies of mammalian CMs demonstrated that the cell-cycle entry can have different outcomes namely polyploidization, binucleation or cell division (Ahuja et al., 2007; Zebrowski and Engel, 2013). Although it is assumed that the cell division is the major response of zebrafish CMs to achieve complete heart regeneration, our study indicates that the polyploidization could partially be a proliferative endpoint of the cycling CMs. The

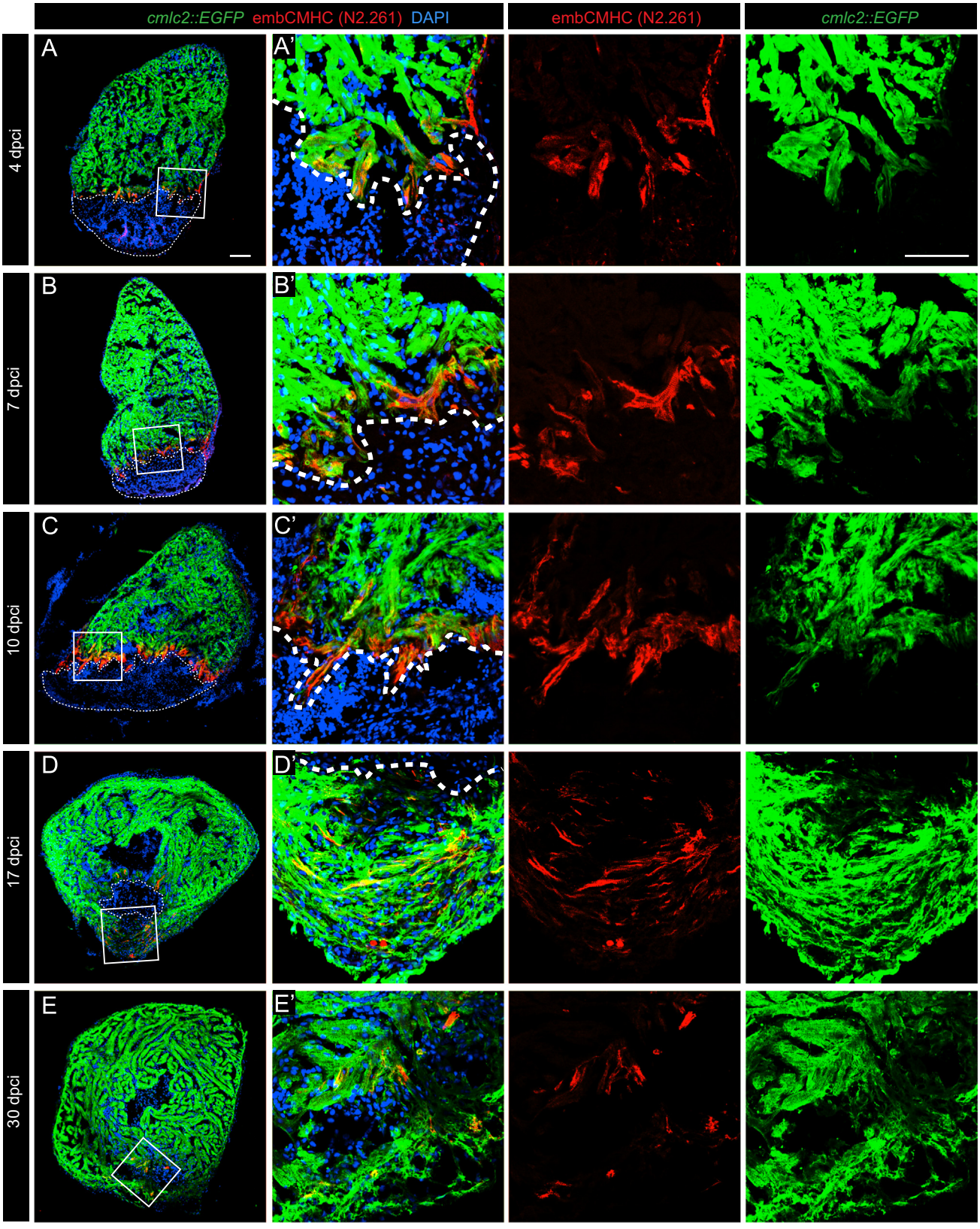

Fig. 5. N2.261 immunostaining reveals a reactivation of embCMHC expression at the vicinity of the post-infarcted tissue. (A–E) Representative images of *cmlc2::EGFP* hearts at different time points during regeneration. Post-infarcted tissue is encircled by a dashed line. (A'–E') Higher magnifications of the framed areas shown in (A-E). EmbCMHC (red) expression was detected only in the vicinity of the cryoinjury border, where CMs dedifferentiate and reduce *cmlc2* expression. At 4 dpci (A), a few scattered embCMHC-positive cells emerge along the injury. At 7 (B) and 10 (C) dpci, the embCMHC-positive cells form a continuous zone above the post-infarcted tissue. At 17 dpci (D), embCMHC-positive cells intermingle with the mature CMs. At 30 dpci (E) only few embCMHC- positive cells are present within the new myocardium. Scale bar (A, A')=100 μm.

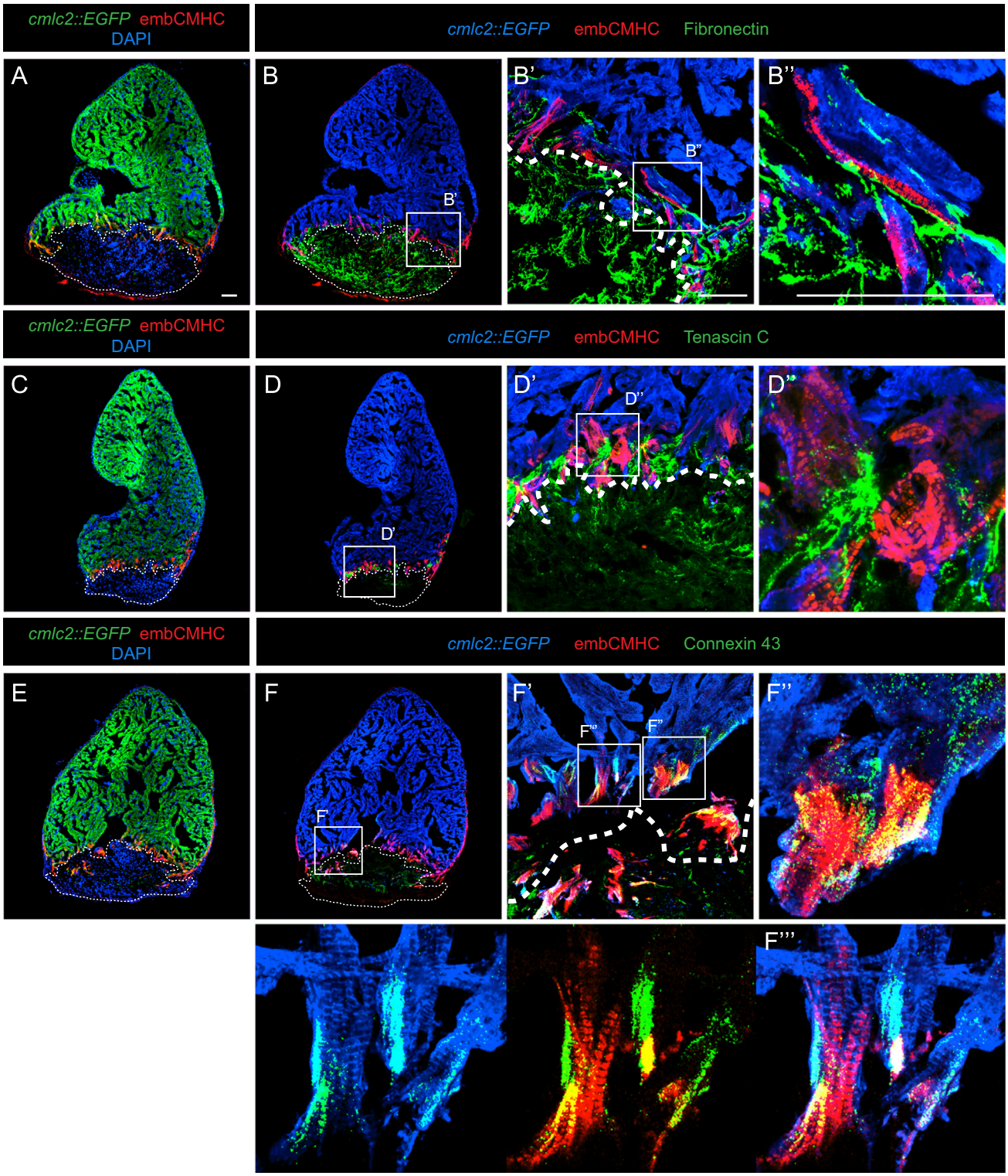

Fig. 6. EmbCMHC-expressing CMs integrate with both the provisional fibrotic tissue and mature myocardium. (A–F) Sections of *cmlc2::EGFP* hearts at 7 dpci immunostained with antibody against Fibronectin (A,B), Tenascin C (C,D) and Connexin 43 (E,F). The post-infarcted tissue (PIT) is encircled with dashed line. (B'–F") Higher magnifications of the framed areas in the left panels. EmbCMHC-positive cells are embedded in the network of the extracellular matrix (ECM) fibers (green) produced by the fibrotic tissue at the myocardial border (B'–D"). (F',F"') The tight junctions protein, Connexin 43, is strongly upregulated in the juxtaposed mature (embCMHC-negative) and undifferentiated (embCMHC-positive) CMs, indicating the electrical coupling between both types of myocytes. Scale bar (A, B', B")=50 μm.

potential hypertrophic response has not yet been addressed in the zebrafish heart, and the percentage of polyploidal CMs in uninjured and regenerated myocardium is unknown. The analysis of the cyclically expressed proteins will be required to determine any differential regulation of cell cycle checkpoints during homeostatic tissue renewal and injury-dependent regeneration.

Recent genetic studies provided clear evidence that the regenerated myocardium derives from the proliferating pre-existing CMs

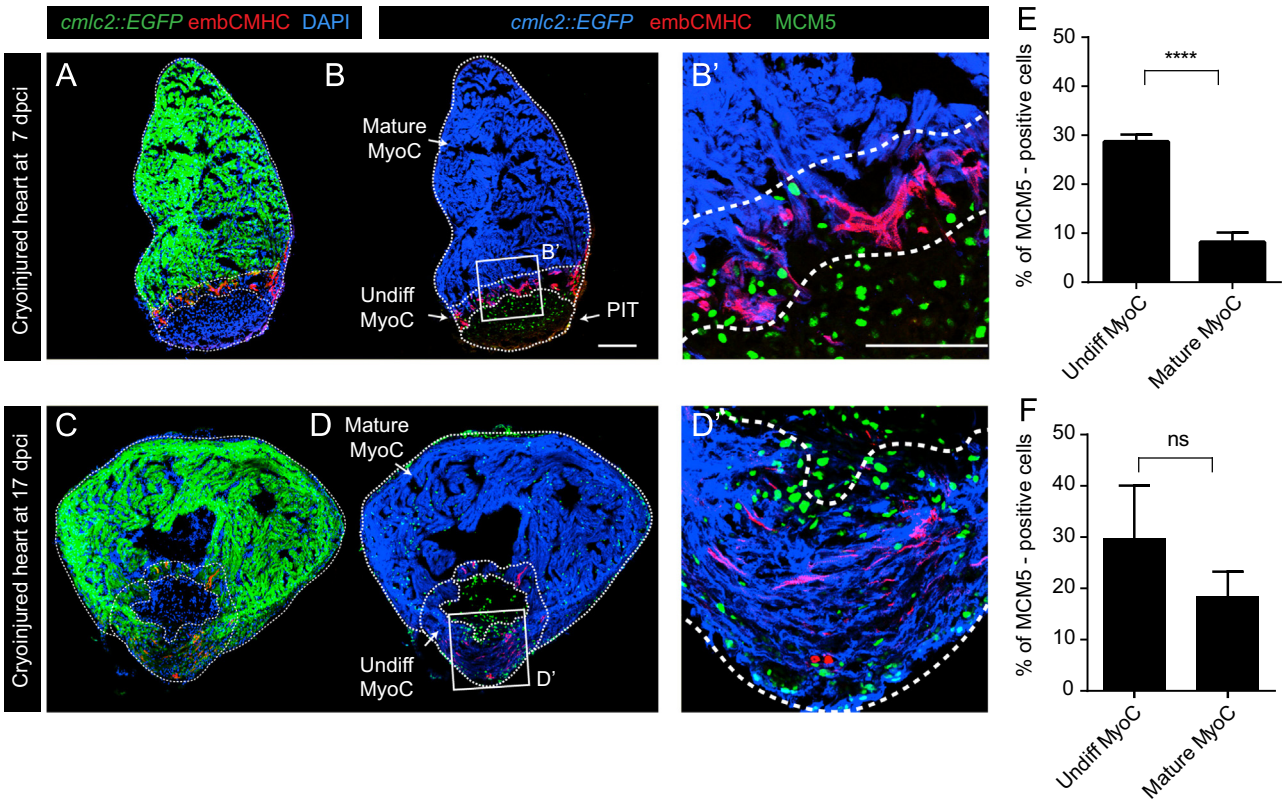

Fig. 7. Undifferentiated CMs display a higher proliferation rate than the mature CMs of the regenerating myocardium. (A–D) Representative images of *cmlc2::EGFP* hearts at 7 (A, B) and 17 (C, D) dpci. Post-infarcted tissue (PIT), undifferentiated myocardium (undiff. MyoC, embCMHC-positive, red) and mature myocardium (mature MyoC, embCMHC-negative) are encircled with a dashed line. Proliferating MCM5-positive cells were normalized to DAPI in each of the compartments. (B') Higher magnification of the framed image in (B). A large accumulation of proliferating cells was observed in the undifferentiated myocardium compartment in comparison to the mature myocardium at 7 dpci. Scale bar (B, B')=100 μm. (E, F) Quantification of MCM5-positive cells reveals a significant increase in the proportion of proliferating cells in the undifferentiated myocardium as compared to mature myocardium at 7 dpci. At 17 dpci, the number of MCM5-positive cells is similar in both myocardial compartments. All results are expressed as the mean ± standard error of the mean (S.E.M.) ($n \geq 3$ hearts, **** *P*-value < 0.0001).

(Jopling et al., 2010; Kikuchi et al., 2010). In this study, we applied two strategies for elucidating the mode of heart regeneration in zebrafish. In the first step, cardiac proliferation/mitotic events were mapped with respect to the injury border in order to discriminate between epimorphic/local and compensatory/global activation of the ventricle at different phases of heart restoration. Then, we defined the differentiation level of the proliferative CMs based on the expression of the embryonic myosin heavy chain isoform.

Epimorphic regeneration involves the formation of a pool of undifferentiated cells underneath the wound healing tissue. Accordingly, we identified a creation of undifferentiated cardiac cells at the interface between the post-infarcted tissue and the intact myocardium. These cells reactivated the expression of sarcomeric protein, called embryonic myosin heavy chain (embCMHC), which is normally expressed in the ventricle during embryogenesis. This myosin isoform may permit the modification of the sarcomere structure providing a higher cellular plasticity that is needed for proliferation, migration and morphogenesis (Maggs et al., 2000). It is interesting to note that the cluster of embCMHC-expressing cells was confined to the distance of 100 μm from the injury site, which corresponds to the similar spatial domain that was reported for mesenchymal dedifferentiation during epimorphic fin regeneration (Akimenko et al., 2003; Poss et al., 2003; Santamaria et al., 1996). This correlation strongly suggests the existence of similar mechanisms and factors in both the fin and the heart, which spread from the injury site to promote cellular dedifferentiation of the abutting stump tissues.

Like in vertebrate appendage regeneration, the population of undifferentiated CMs was established at the initial phase of regeneration immediately after wound healing, which in the zebrafish heart corresponds to 4–10 dpci. While regeneration was progressing, the expression of embCMHC started to disperse and decline, and it almost disappeared at the termination phase at 30 dpci. The group of undifferentiated CM domains can be considered as a cardiac blastema according to their features, such as the reactivation of the embryonic tissue-specific gene, higher proliferative index, the localization at the edge of the injury, the association with the wound tissue and functional integration with the original tissue. Like in the classical epimorphic regeneration, the damaged structure is nearly perfectly reproduced, and after the completion of regeneration, the border between the original and new myocardium cannot be distinguished by means of the histological or immunohistochemistry methods. The presence of the cardiac blastema and the accuracy of tissue replacement support a model of heart regeneration in which the initiation of cardiac regeneration predominantly has an epimorphic character (Fig. 8).

Although the expression of embCMHC was restricted to the highly proliferative blastema, enhanced cell proliferation was detected throughout the entire intact myocardium beyond the 100–200 μm zone from the fibrotic tissue-myocardium border. The graphical map of all individual mitotic CMs displayed differences and similarities between the initial and progressive phases of heart regeneration. The major difference was that at 7 dpci, 70% of PH3-positive CMs were located in the proximity of the injury zone up to 200 μm, as opposed to 17 dpci, where mitotic CMs were uniformly distributed in the whole ventricle. Thus, the peak of blastema cell proliferation can be detected only during the initiation phase. Despite this variation, we also observed similarities between the early and late regeneration phases, mainly concerning the activation of the intact myocardium.

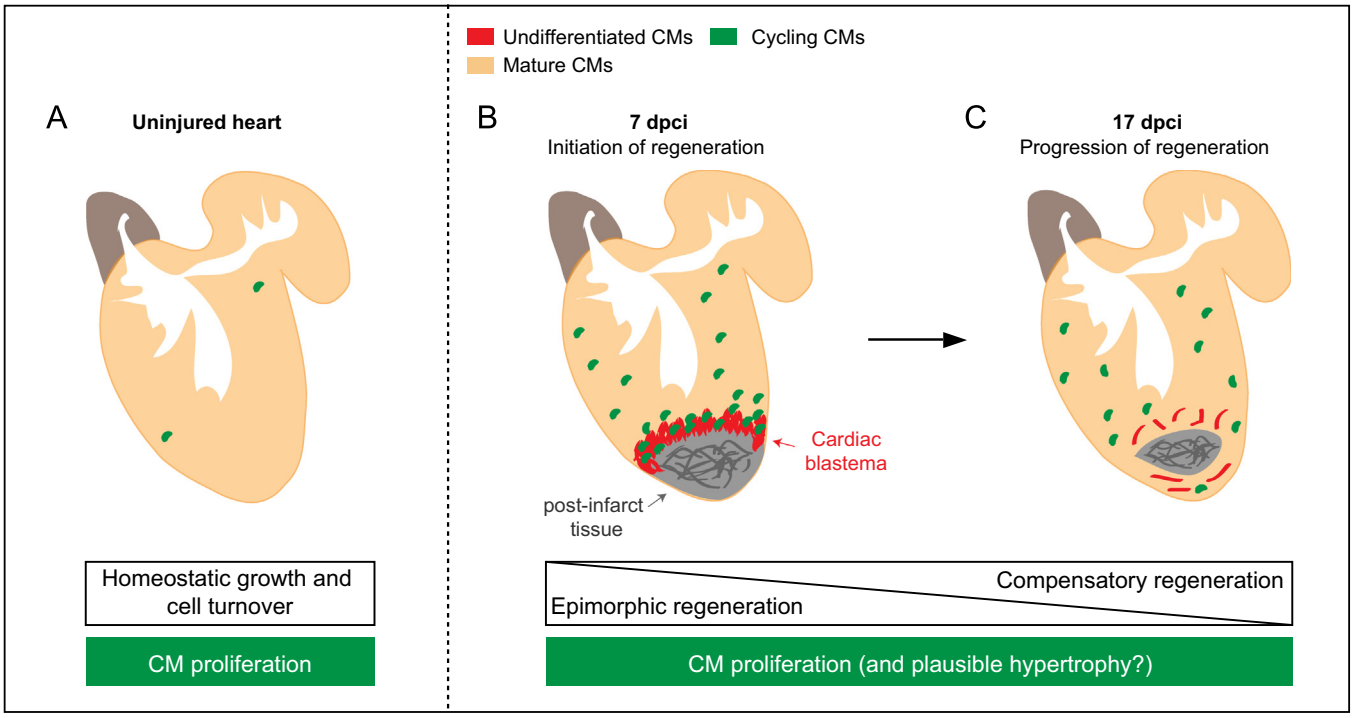

Fig. 8. Restoration of the zebrafish heart after cryoinjury is accomplished by a combination of local epimorphic and global compensatory modes of regeneration. (A) In the uninjured adult heart, few CMs undergo cell division to ensure a slow homeostatic tissue turnover. (B) The initial phase of heart regeneration involves a formation of a cardiac blastema at the wound site, which is a hallmark of epimorphic regeneration. These undifferentiated proliferating CMs are, from one side, attached to the ECM network of the fibrotic tissue, and from the other side, they form tight-junction connections with the mature CMs. In parallel, the mature myocardium activates compensatory cell proliferation at the organ level. (C) As regeneration progresses, the fibrotic tissue is progressively replaced with a new cardiac tissue. Cardiac blastema cells differentiate and become integrated with the mature myocardium. Compensatory proliferative response of the entire ventricle continues to reinforce the initial epimorphic cardiac regeneration.

At both time points, PH3-positive CMs were evenly distributed in the organ-wide range, suggesting an absence of a mitogenic gradient from the wound tissue across the remote remaining myocardium. This even distribution of PH3-positive cells argues for a systemic mechanism that triggers proliferation in the entire myocardium. The current work did not test what is the physiological significance of the global proliferative response. The role of the compensatory mode of regeneration has to be addressed in the future. In our previous study, electrocardiogram analyses have demonstrated that the local cryoinjury affects the contractile heart function (Chablais et al., 2011). The compensatory response may represent a suitable strategy to cope with the physiological defect of the life essential organ while conceding time to the local epimorphic regenerative process. The compensatory regeneration typically involves hyperplasia, which is independent of the reactivation of embryonic structural proteins. This mode of regeneration confirms the notion that dedifferentiation is not a prerequisite for cell cycle re-entry (Engel, 2005; Zebrowski and Engel, 2013). Thus, we can propose a model, in which cryoinjury initially triggers a local epimorphic regenerative response, which is reinforced by a compensatory regeneration within the entire remaining organ (Fig. 8). Further studies are required to investigate whether the stress of injury could in addition stimulate cardiac hypertrophy, which would provide a valuable model for regenerative medicine.

In this study, we focused on the basic principles of heart regeneration in zebrafish, without addressing the nature of the inductive mechanisms. Our main goals were to provide a comprehensive statistical analysis of proliferating CMs and to map these cells with respect to the injury, in order to understand the source of the mitogens in the myocardium. One of them must be in the post-infarcted tissue, in particular during the initial phase of regeneration. The identification of cardiac mitogens remains one of the big challenges in the field. Previous studies have suggested that several signaling molecules such as TGF-β, FGF or retinoic acid act mostly at the short-range level to stimulate CMs proliferation, although their global activity in the intact myocardium is not ruled out (Chablais and Jazwinska, 2012b; Kikuchi et al., 2011; Lepilina et al., 2006). In addition to the classical signaling pathways, it must be addressed whether mechanical, hormonal and cytokine stimuli are involved in the regulation of the compensatory response. In conclusion, we have demonstrated a diversity of the regenerative mechanisms in the zebrafish heart that requires further considerations in the future analysis.

Materials and methods

Animal procedures

The present work was performed with adult fish at the age of 9–18 months. Wild type fish were AB (Oregon), transgenic fish were *cmlc2::DsRed2-Nuc* (Rottbauer et al., 2002) and *cmlc2::EGFP* zebrafish strains (Burns et al., 2005). Cryoinjuries were performed as described previously (Chablais and Jazwinska, 2012a; Chablais et al., 2011). Ventricular resections were done as described previously (Poss et al., 2002). For bromodeoxyuridine (BrdU) incorporation experiments, the animals were maintained in 5 mg/ml BrdU (B5002, Sigma-Aldrich) for 21 days, the fish were daily fed, and the solution was changed every second day. The experimental research on animals was approved by the cantonal veterinary office of Fribourg.

Immunohistochemistry

At the end of each experiment, the hearts were collected and fixed overnight at 4 °C in 2% paraformaldehyde. They were then rinsed in PBS and equilibrated in 30% sucrose before embedding

in Tissue-Tek OCT compound (Sakura Finetek Europe B.V.) and cryosectioned at a thickness of 16 μm.

The immunohistochemistry procedures were performed as described previously (Chablais et al. 2011). The following primary antibodies were used: mouse anti-tropomyosin at 1:100 (developed by J. Jung-Chin Lin and obtained from Developmental Studies Hybridoma Bank, CH1), rabbit anti-MCM5 at 1:5000 (provided by Soojin Ryu), chicken anti-GFP at 1:2000 (Aves Labs, GFP-1010), mouse anti-p-Histone 3 at 1:200 (Clone 3H10, Millipore), rabbit anti-tubulin gamma at 1:2000 (Abcam, ab11321), rabbit anti-DsRed (Clonetech, 632496) at 1:200, mouse anti-N2.261 (developed by H.M. Blau, obtained from Developmental Studies Hybridoma Bank) at 1:50 and rat anti-BrdU at 1:100 (Abcam, ab6326). For the BrdU immunostaining, the slides were incubated in 2N HCl in PBS with 0.3% Triton during 45 min before the immunohistochemistry procedure. The Alexa-Fluor-conjugated secondary antibodies (Jackson Immunoresearch) were used at 1:500, and DAPI was used at 1:2000.

Image analysis and quantification

After antibody staining, cardiac tissue imaging was performed at different magnifications (20 × and 63 ×) with confocal microscopes (Leica TCS-SP5 and Leica TCS-SPE-II). ImageJ software was used to perform the subsequent image analysis. To quantify the number of proliferating CMs, the images of cell-cycle markers (MCM5, PH3, BrdU) were overlapped with the images of CM markers (*cmlc2::EGFP* immunostained with anti-GFP antibody; *cmlc2::DsRed2-nuc* immunostained with anti-DsRed antibody). The total number of proliferating cells was obtained by overlapping the fluorescent signals of the cell-cycle markers with DAPI. Results for the non-CM populations were obtained by subtracting the data acquired for CMs from the ones acquired for the total cell number. The cells positive for MCM5, PH3 or BrdU were quantified in several subsequent sections (from 4 to 10 sections of cryoinjured hearts, and from 6 to 16 sections of the uninjured heart) and pulled together to obtain the total number of specific cells per heart. The cryoinjured area was calculated as a percentage of the entire area of the ventricular sections. The relative localization of PH3-positive CMs was obtained by measuring the shortest distance between each of the cells and the CI border. The relative localization of BrdU-positive CMs was determined in the myocardial zones at the step-size distance of 100 μm from the CI border. In order to obtain a representative data for each of the hearts, we imaged and analyzed several nonadjacent sections with a space of at least 80 μm between them. Because the mitotic events were very rare in the uncut heart, we had to analyse nearly all the heart sections in order to determine the number of PH3-positive cells.

To enhance the visibility of the blue fluorescent color on the final figures, we modified the color profile with Adobe Photoshop using CMYK conversion.

Acknowledgments

We thank V. Zimmermann for excellent technical assistance and for fish care; F. Chablais for specimen, and Dr. Pierre Aeby for critical reading of the manuscript. This work was supported by the Swiss National Science Foundation, Grant numbers: 310030_138062 and CRSII3_147675 and the Schweizerische Stiftung für die Erforschung der Muskelkrankheiten.

Appendix A. Supporting information

Supplementary data associated with this article can be found in the online version at http://dx.doi.org/10.1016/j.ydbio.2014.12.002.

References

Ahuja, P., Sdek, P., MacLellan, W.R., 2007. Cardiac myocyte cell cycle control in development, disease, and regeneration. Physiol. Rev. 87, 521–544.
Akimenko, M.A., Mari-Beffa, M., Becerra, J., Geraudie, J., 2003. Old questions, new tools, and some answers to the mystery of fin regeneration. Dev. Dyn. 226, 190–201.
Ausoni, S., Sartore, S., 2009. From fish to amphibians to mammals: in search of novel strategies to optimize cardiac regeneration. J. Cell Biol. 184, 357–364.
Beltrami, A.P., Urbanek, K., Kajstura, J., Yan, S.M., Finato, N., Bussani, R., Nadal-Ginard, B., Silvestri, F., Leri, A., Beltrami, C.A., Anversa, P., 2001. Evidence that human cardiac myocytes divide after myocardial infarction. N. Engl. J. Med. 344, 1750–1757.
Bergmann, O., Bhardwaj, R.D., Bernard, S., Zdunek, S., Barnabe-Heider, F., Walsh, S., Zupicich, J., Alkass, K., Buchholz, B.A., Druid, H., Jovinge, S., Frisen, J., 2009. Evidence for cardiomyocyte renewal in humans. Science 324, 98–102.
Brockes, J.R., Kumar, A., 2008. Comparative aspects of animal regeneration. Annu. Review Cell Dev. Biol. 24, 525–549.
Burns, C.G., Milan, D.J., Grande, E.J., Rottbauer, W., MacRae, C.A., Fishman, M.C., 2005. High-throughput assay for small molecules that modulate zebrafish embryonic heart rate. Nat. Chem. Biol. 1, 263–264.
Carlson, B.M., 2007. Principles of Regenerative Biology. Elsevier/Academic Press, Amsterdam; Burlington, Mass.
Chablais, F., Jazwinska, A., 2012a. Induction of myocardial infarction in adult zebrafish using cryoinjury. J. Vis. Exp..
Chablais, F., Jazwinska, A., 2012b. The regenerative capacity of the zebrafish heart is dependent on TGFbeta signaling. Development 139, 1921–1930.
Chablais, F., Veit, J., Rainer, G., Jazwinska, A., 2011. The zebrafish heart regenerates after cryoinjury-induced myocardial infarction. BMC Dev. Biol. 11, 21.
Curado, S., Stainier, D.Y., 2006. The HeArt of regeneration. Cell 127, 462–464.
Engel, F.B., 2005. Cardiomyocyte proliferation: a platform for mammalian cardiac repair. Cell Cycle 4, 1360–1363.
Gonzalez-Rosa, J.M., Martin, V., Peralta, M., Torres, M., Mercader, N., 2011. Extensive scar formation and regression during heart regeneration after cryoinjury in zebrafish. Development 138, 1663–1674.
Hans, F., Dimitrov, S., 2001. Histone H3 phosphorylation and cell division. Oncogene 20, 3021–3027.
Jazwinska, A., Ehler, E., Hughes, S.M., 2003. Intermediate filament-co-localized molecules with myosin heavy chain epitopes define distinct cellular domains in hair follicles and epidermis. BMC Cell Biol. 4, 10.
Jopling, C., Boue, S., Izpisua Belmonte, J.C., 2011. Dedifferentiation, transdifferentiation and reprogramming: three routes to regeneration. Nat. Rev. Mol. Cell Biol. 12, 79–89.
Jopling, C., Sleep, E., Raya, M., Marti, M., Raya, A., Izpisua Belmonte, J.C., 2010. Zebrafish heart regeneration occurs by cardiomyocyte dedifferentiation and proliferation. Nature 464, 606–609.
Kikuchi, K., Holdway, J.E., Major, R.J., Blum, N., Dahn, R.D., Begemann, G., Poss, K.D., 2011. Retinoic acid production by endocardium and epicardium is an injury response essential for zebrafish heart regeneration. Dev. Cell 20, 397–404.
Kikuchi, K., Holdway, J.E., Werdich, A.A., Anderson, R.M., Fang, Y., Egnaczyk, G.F., Evans, T., Macrae, C.A., Stainier, D.Y., Poss, K.D., 2010. Primary contribution to zebrafish heart regeneration by gata4(+) cardiomyocytes. Nature 464, 601–605.
Kikuchi, K., Poss, K.D., 2012. Cardiac regenerative capacity and mechanisms. Annu. Rev. Cell Dev. Biol. 28, 719–741.
Knockleby, J.W., Lee, H., 2010. Same partners, different dance Involvement of DNA replication proteins in centrosome regulation. Cell Cycle 9, 4487–4491.
Kollman, J.M., Merdes, A., Mourey, L., Agard, D.A., 2011. Microtubule nucleation by gamma-tubulin complexes. Nat. Rev. Mol. Cell Biol. 12, 709–721.
Kubin, T., Poling, J., Kostin, S., Gajawada, P., Hein, S., Rees, W., Wietelmann, A., Tanaka, M., Lorchner, H., Schimanski, S., Szibor, M., Warnecke, H., Braun, T., 2011. Oncostatin M is a major mediator of cardiomyocyte dedifferentiation and remodeling. Cell Stem Cell 9, 420–432.
Lajoie-Mazenc, I., Tollon, Y., Detraves, C., Julian, M., Moisand, A., Gueth-Hallonet, C., Debec, A., Salles-Passador, I., Puget, A., Mazarguil, H., et al., 1994. Recruitment of antigenic gamma-tubulin during mitosis in animal cells: presence of gamma-tubulin in the mitotic spindle. J. Cell Sci. 107 (Pt 10), 2825–2837.
Laube, F., Heister, M., Scholz, C., Borchardt, T., Braun, T., 2006. Re-programming of newt cardiomyocytes is induced by tissue regeneration. J. Cell Sci. 119, 4719–4729.
Lepilina, A., Coon, A.N., Kikuchi, K., Holdway, J.E., Roberts, R.W., Burns, C.G., Poss, K.D., 2006. A dynamic epicardial injury response supports progenitor cell activity during zebrafish heart regeneration. Cell 127, 607–619.
Liu, J., Bressan, M., Hassel, D., Huisken, J., Staudt, D., Kikuchi, K., Poss, K.D., Mikawa, T., Stainier, D.Y., 2010. A dual role for ErbB2 signaling in cardiac trabeculation. Development 137, 3867–3875.
Maggs, A.M., Taylor-Harris, P., Peckham, M., Hughes, S.M., 2000. Evidence for differential post-translational modifications of slow myosin heavy chain during murine skeletal muscle development. J. Muscle Res. Cell Motil. 21, 101–113.
Major, R.J., Poss, K.D., 2007. Zebrafish heart regeneration as a model for cardiac tissue repair. Drug Discov. Today. Dis. Models 4, 219–225.
Poss, K.D., 2007. Getting to the heart of regeneration in zebrafish. Semin. Cell Dev. Biol. 18, 36–45.
Poss, K.D., Keating, M.T., Nechiporuk, A., 2003. Tales of regeneration in zebrafish. Dev. Dyn.: Off. Publ. Am. Assoc. Anat. 226, 202–210.

Poss, K.D., Wilson, L.G., Keating, M.T., 2002. Heart regeneration in zebrafish. Science 298, 2188–2190.
Rajabi, M., Kassiotis, C., Razeghi, P., Taegtmeyer, H., 2007. Return to the fetal gene program protects the stressed heart: a strong hypothesis. Heart Fail. Rev. 12, 331–343.
Rottbauer, W., Saurin, A.J., Lickert, H., Shen, X., Burns, C.G., Wo, Z.G., Kemler, R., Kingston, R., Wu, C., Fishman, M., 2002. Reptin and pontin antagonistically regulate heart growth in zebrafish embryos. Cell 111, 661–672.
Santamaria, J.A., Mari-Beffa, M., Santos-Ruiz, L., Becerra, J., 1996. Incorporation of bromodeoxyuridine in regenerating fin tissue of the goldfish Carassius auratus. J. Exp. Zool. 275, 300–307.
Schnabel, K., Wu, C.C., Kurth, T., Weidinger, G., 2011. Regeneration of cryoinjury induced necrotic heart lesions in zebrafish is associated with epicardial activation and cardiomyocyte proliferation. Plos One 6.
Singh, B.N., Koyano-Nakagawa, N., Garry, J.P., Weaver, C.V., 2010. Heart of newt: a recipe for regeneration. J. Cardiovasc. Transl. Res. 3, 397–409.
Soonpaa, M.H., Field, L.J., 1998. Survey of studies examining mammalian cardiomyocyte DNA synthesis. Circ. Res. 83, 15–26.
Soonpaa, M.H., Rubart, M., Field, L.J., 2013. Challenges measuring cardiomyocyte renewal. Biochim. Biophys. Acta 1833, 799–803.
Szibor, M., Poling, J., Warnecke, H., Kubin, T., Braun, T., 2014. Remodeling and dedifferentiation of adult cardiomyocytes during disease and regeneration. Cell. Mol. Life Sci. 71, 1907–1916.
Taegtmeyer, H., Sen, S., Vela, D., 2010. Return to the fetal gene program: a suggested metabolic link to gene expression in the heart. Ann. NY Acad. Sci. 1188, 191–198.
Yelon, D., 2012. Developmental biology: heart under construction. Nature 484, 459–460.
Zebrowski, D.C., Engel, F.B., 2013. The cardiomyocyte cell cycle in hypertrophy, tissue homeostasis, and regeneration. Rev. Physiol. Bioch. Pharmacol. 165, 67–96.
Zhang, R., Han, P., Yang, H., Ouyang, K., Lee, D., Lin, Y.F., Ocorr, K., Kang, G., Chen, J., Stainier, D.Y., Yelon, D., Chi, N.C., 2013. In vivo cardiac reprogramming contributes to zebrafish heart regeneration. Nature 498, 497–501.